Visual Tracking Control of a Wheeled Mobile Robot With System Model and Velocity Quantization Robustness

Chi-Yi Tsai and Kai-Tai Song, *Associate Member, IEEE*

***Abstract*—This paper presents a visual tracking control design of a nonholonomic mobile robot equipped with a tilt camera. The proposed design enhances various image-tracking applications using an on-board monocular camera, such as human-robot interaction and surveillance. Based on Lyapunov theory, the proposed control scheme not only possesses some degree of robustness against parametric uncertainty, but also overcomes the external uncertainty caused by velocity quantization noise. Moreover, the proposed controller fully works in the image space; hence, the computational complexity and the effects of sensor/camera modeling errors can be greatly reduced. Experimental results validate the effectiveness of the proposed control scheme, in terms of tracking performance, system convergence, and robustness.**

***Index Terms*—Parametric uncertainty, round-off error, uniform quantization error, visual tracking control, wheeled mobile robots.**

I. Introduction

ONE OF THE important features in designing intelligent service robots, such as exhibition guide robots or elderly-care robots, is to make the robot interact naturally with people. The key factors to accomplish such human-robot interactive task encompass several research topics, such as face detection, voice recognition, visual tracking, etc. With visual tracking, a robot can focus attention to a user and interact with him/her accordingly. Hence, the research on visual tracking control of mobile robots has been an active area in robotics and computer vision [1]–[14].

Mobile robots with two independent driving wheels are widely adopted for home or service robotic platforms. These robots are nonholonomic and their motion is controlled by only two control inputs under the nonholonomic constraint. Existing visual servo control results for holonomic manipulators are not suitable for such mobile platforms. In recent years, the study of visual tracking control of nonholonomic mobile robots equipped with an on-board monocular camera to track a target has gained increasing attention. The reported methods usually focus on the visual tracking control of wheeled mobile robots to track a static target, such as a ground line, landmark, or reference image, for the purpose of visual navigation [1]–[4] or visual regulation [5]–[8]. On the other hand, because tracking a dynamic moving target is an important requirement for intelligent robotics, some efforts focused on the control problem of visual tracking of a dynamic moving (non-static) target. In [9], Wang *et al.* proposed an adaptive backstepping control law based on an image-based camera-target visual interaction model to track a moving target with unknown height parameter. Although their approach guarantees asymptotic stability of the closed-loop visual tracking system in tracking a moving target, the case of tracking a static target cannot be guaranteed due to the nonzero restrictions on the reference velocity of the mobile robot. In [10], Song *et al.* combined a face detection algorithm with a proportional–integral–derivative (PID) controller to track a moving person in a home setting. The main disadvantage of their method is that it cannot guarantee the stability of the closed-loop visual tracking system based on a stability criterion. In [11], Malis *et al.* integrated template-based visual tracking algorithms and model-free vision-based control techniques to build a flexible and robust visual tracking control system for various robotic applications. The reported system failed in the full occlusion condition due to the requirement of homography estimation. In [12], Han *et al.* proposed an image-based visual tracking control scheme for a mobile robot to estimate the position of the target in the next image and track the target to the central area of the image; however, the estimation result was very sensitive to the image noise due to the shortcoming of the differential approximation approach.

From the literature, it is still a challenge to design a robust visual tracking controller for nonholonomic mobile robots to track a dynamic moving target based on a stability criterion. Further, in realization of the control schemes, it has been noted that the disturbances of velocity quantization error and target occlusion degrade the performance of the controller and might make the system unstable. These problems have not yet been clarified in many existent related works and hence motivated us to develop a robust visual tracking control method to overcome uncertainties of system model, velocity quantization, and occlusion. To achieve this, a visual tracking controller with velocity quantization robustness has been proposed in the authors' previous work [13]. Recently, the authors combined a self-tuning Kalman filter with the visual tracking controller to estimate the target motion velocity and overcome the occlusion uncertainty [14]. However, in order to handle practical visual tracking situations

Manuscript received May 15, 2007; revised August 10, 2007 and April 07, 2008. Manuscript received in final form May 22, 2008. First published December 09, 2008; current version published April 24, 2009. Recommended by Associate Editor B. de Jager. This work was supported in part by the National Science Council of Taiwan under Grant NSC 94-2218-E-009-008 and by the Ministry of Economic Affairs under Grant 95-EC-17-A-04-S1-054.

C.-Y. Tsai is with the Department of Electrical and Control Engineering, National Chiao Tung University, Hsinchu 300, Taiwan, and also with the Software R&D Department, EPC Business Unit, ASUSTek Computer Incorporation, Taipai 112, Taiwan (e-mail: chiyi.ece91g@nctu.edu.tw).

K.-T. Song is with the Department of Electrical and Control Engineering, National Chiao Tung University, Hsinchu 300, Taiwan (e-mail: ktsong@mail.nctu.edu.tw).

Color versions of one or more of the figures in this paper are available online at http://ieeexplore.ieee.org.

Digital Object Identifier 10.1109/TCST.2008.2001053

and guarantee the stability of the closed-loop visual tracking system, the parametric uncertainty in system model requires urgent attention. Therefore, this paper extends the previous study [13] to analyze the robustness property against the system model uncertainty.

The rest of this paper is organized as follows. Section II describes the system modeling of visual tracking control problem and the controller design accordingly. In Section III, the robustness of the control system against the system model uncertainty is analyzed and discussed. Section IV presents the design of the robust control law to overcome the velocity quantization error encountered in practical systems. Experimental results are reported in Section V. Several interesting experimental observations will be presented and discussed. Section VI concludes the contributions of this paper.

II. System Modeling and Controller Design

We consider the nonholonomic visual tracking control problem such that a wheeled mobile robot with a tilt camera tracks a dynamic moving target, which is supposed to be a well-recognizable object with appropriate dimensions in the image plane and can only translate with respect to the robot. For instance, a cylindrical target as shown in Fig. 2 was used in the experiments of this paper, and a human face was tracked as a target in [13]. The tilt camera is mounted on top of the mobile robot and is assumed to have a limited field of view. Fig. 1(a) illustrates a model of the wheeled mobile robot and the target in the world coordinate frame F_f, in which the target motion is supposed to be holonomic but with only translational motion relative to the robot. Fig. 1(b) is the side view of the scenario under consideration, in which the distance δy and tilt angle ϕ give the relation between the camera coordinate frame F_c and the mobile coordinate frame F_m. In order for the mobile robot to interact with the target in the image coordinate frame F_i, a visual interaction model was proposed in [13]. Fig. 2 shows the definition of system state in F_i. In Fig. 2, x_i and y_i are, respectively, the horizontal and vertical position of the centroid of target in the image plane, and d_x is the width of target in the image plane. Setting $X_i = [\,x_i \quad y_i \quad d_x\,]^T$ to denote the system state, the linearized visual interaction model can be derived by quasi-linear parameter-varying (Quasi-LPV) description [15] such that

$$\dot{X}_i = \mathbf{A}_i\left(V_f^t, \phi, \theta_f^m\right) X_i + \mathbf{B}_i(X_i, \phi)u + C_i\left(V_f^t, \phi, \theta_f^m\right) \quad (1)$$

where $V_f^t = [\,v_f^x \quad v_f^y \quad v_f^z\,]^T$ is the target velocity in Cartesian coordinates, $\left(\theta_f^m, \phi\right)$ are the orientation angle of the mobile robot and the tilt angle of the on-board camera. We define two scalars $k_x = d_x/W$ and $k_y = k_x f_y/f_x$, where W denotes the actual width of the target, (f_x, f_y) represent the fixed focal length along the image x-axis and y-axis, respectively. We denote $\left(v_f^m, w_f^m\right)$ the linear and angular velocity of the mobile robot, w_t^m the tilt velocity of the camera, and diag() a 3×3 diagonal matrix, then the matrices $(\mathbf{A}_i, \mathbf{B}_i)$ and vectors $(u, \mathbf{C}_i)$ defined in (1) are given by the equation shown at the bottom of the page.

Based on the visual interaction model (1), a feedback linearization control law can be derived as in [13]

$$u = \mathbf{B}_i^{-1}(\mathbf{K}_g X_e - \mathbf{A}_i \overline{X}_i - C_i) \quad (2)$$

where $\mathbf{K}_g = \mathrm{diag}(\alpha_1 + A_1, \alpha_2 + A_2, \alpha_3 + A_1)$ is an 3×3 gain matrix, in which $(\alpha_1, \alpha_2, \alpha_3)$ are three positive scalar factors, $X_e = \overline{X}_i - X_i$ is the error-state in the image plane, and $\overline{X}_i = [\,\overline{x}_i \quad \overline{y}_i \quad \overline{d}_x\,]^T$ is the fixed desired state in the image plane.

Note that the control law (2) poses a singularity problem of matrix $\mathbf{B}_i$. As shown in Fig. 3, (x_c, y_c, z_c) represents the target position with respect to the camera in the camera coordinate frame and ϕ' is the angle related to the location of the target. The singularity condition of matrix $\mathbf{B}_i$ can be found such that (readers refer to [13] for detailed derivation)

$$\tan\phi = f_y(y_i + S d_x)^{-1} = z_c(y_c + \delta y)^{-1} = \tan(\phi + \phi') \quad (3)$$

where $S = (f_y \delta y)/(f_x W)$ is a scalar. Expression (3) implies that the matrix $\mathbf{B}_i$ becomes singular when ϕ' equals to 0 or π. The physical meaning of this is that the target is directly above or directly below the robot, and the robot will be unable

$$\mathbf{A}_i\left(V_f^t, \phi, \theta_f^m\right) = \mathrm{diag}(A_1, A_2, A_1)$$

$$A_1 = -f_x^{-1} k_x \left(v_f^x \cos\phi \sin\theta_f^m + v_f^y \sin\phi + v_f^z \cos\phi \cos\theta_f^m\right)$$

$$A_2 = -f_y^{-1} k_y \left(v_f^x \cos\phi \sin\theta_f^m + v_f^y \sin\phi + v_f^z \cos\phi \cos\theta_f^m\right)$$

$$\mathbf{B}_i(X_i, \phi) = \begin{bmatrix} f_x^{-1} k_x x_i \cos\phi & f_x^{-1}\left(x_i^2 + f_x^2\right)\cos\phi - f_y^{-1} f_x (k_y \delta y + y_i)\sin\phi & -f_y^{-1} x_i (k_y \delta y + y_i) \\ k_y\left(\sin\phi + f_y^{-1} y_i \cos\phi\right) & f_x^{-1} f_y x_i \left(\sin\phi + f_y^{-1} y_i \cos\phi\right) & -f_y^{-1}\left(y_i^2 + f_y^2 + k_y y_i \delta y\right) \\ f_x^{-1} k_x d_x \cos\phi & f_x^{-1} x_i d_x \cos\phi & -f_y^{-1} d_x (k_y \delta y + y_i) \end{bmatrix}$$

$$C_i\left(V_f^t, \phi, \theta_f^m\right) = \begin{bmatrix} k_x(v_f^z \sin\theta_f^m - v_f^x \cos\theta_f^m) \\ k_y\left(v_f^y \cos\phi - v_f^x \sin\phi \sin\theta_f^m - v_f^z \sin\phi \cos\theta_f^m\right) \\ 0 \end{bmatrix}$$

$$u = \begin{bmatrix} v_f^m \\ w_f^m \\ w_t^m \end{bmatrix}$$

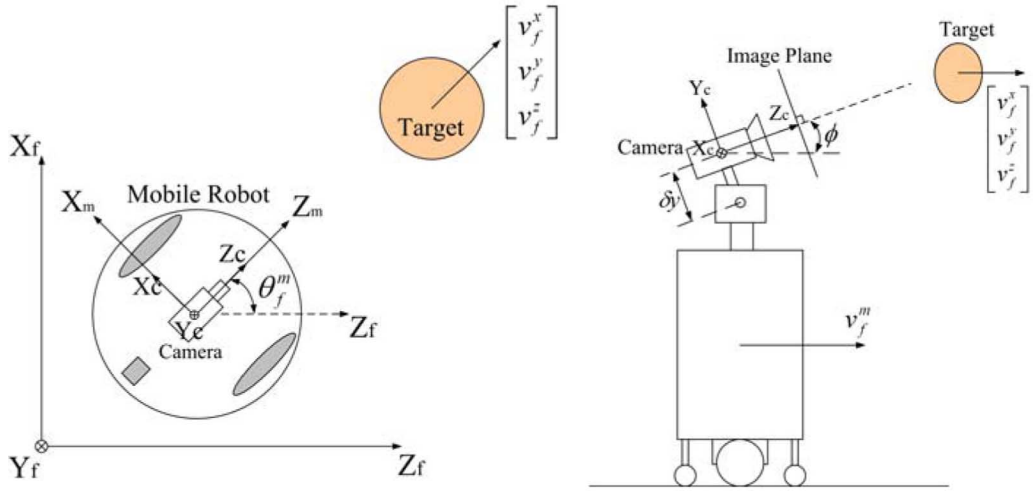

Fig. 1. (a) Model of the wheeled mobile robot and the target in the world coordinate frame. (b) Side view of the wheeled mobile robot with a tilt camera mounted on top of it.

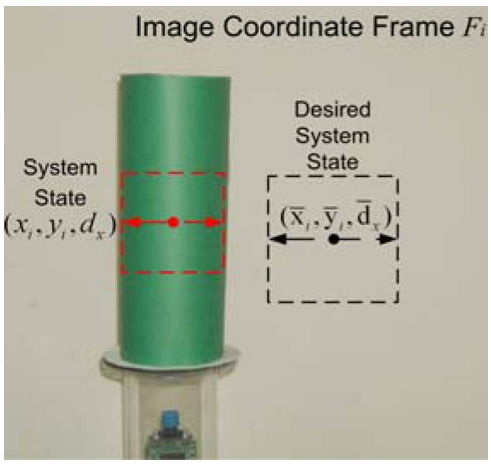

Fig. 2. Definition of system state in the image plane.

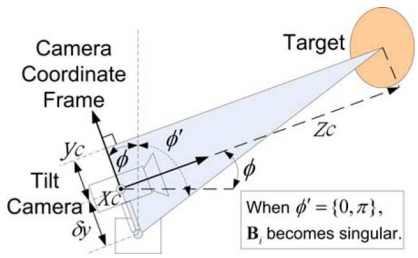

Fig. 3. Physical meaning of the singularity condition (3).

to approach the target in any way due to deficient degree-of-freedom. Therefore, the robot should stop tracking temporarily under such circumstances. Also note that the controller (2) requires the target motion velocity, which can be estimated by a visual state estimator [14]. In this paper, this information is supposed to be known *a priori* in order to verify the performance of the proposed controller design.

Remark 1: The proposed visual interaction model (1) poses a question that the derivation of $d_x = k_x W$ is not always hold

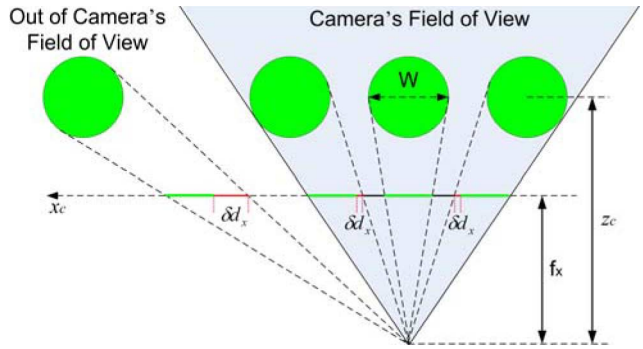

Fig. 4. Derivation error of d_x.

for a cylindrical target used in the system modeling. As shown in Fig. 4, parameters W, f_x, and z_c remain the same, but the cylindrical target is shifted along x_c. The projection d_x is not the same and includes an error δd_x. Because the camera is supposed to be limited field of view, the error δd_x would be small and could be modeled as a system uncertainty. In Section III, the robustness analysis is presented in order to handle this kind of uncertainty.

III. Robustness Against System Model Uncertainty

In this section, the robustness of the visual tracking controller (2) is investigated against model uncertainties from camera parameters (f_x, f_y), robot parameters (θ_f^m, ϕ), target parameters (W, v_f^x, v_f^y, v_f^z), and measurement of system state $d_x = k_x W$. We first define a positive-definite

Lyapunov function

$$V(x_e, y_e, d_e) = \frac{1}{2}\left(x_e^2 + y_e^2 + d_e^2\right). \tag{4}$$

Taking the derivative of (4) yields, where

$$\dot{V} = X_e^T \dot{X}_e = -\left[X_e^T(\mathbf{A}_i X_i + C_i) + X_e^T \mathbf{B}_i u\right] \equiv -f(u) \tag{5}$$

$\dot{X}_e = \mathbf{A}_i X_e - \mathbf{B}_i u - (\mathbf{A}_i \overline{X}_i + C_i)$ is the error-state model of (1). In view of the Lyapunov theory [16], expression (5) tells us that if $f(u) > 0$ then the equilibrium point of the system $\dot{X}_e$ is asymptotically stable. Consider the following system with parametric uncertainties:

$$\begin{aligned}\dot{X}_e &= \overline{\mathbf{A}}_i X_e - \overline{\mathbf{B}}_i u - (\overline{\mathbf{A}}_i \overline{X}_i + \overline{C}_i) \\ &= (\mathbf{A}_i + \delta\mathbf{A}_i) X_e - (\mathbf{B}_i + \delta\mathbf{B}_i) u \\ &\quad - [(\mathbf{A}_i + \delta\mathbf{A}_i)\overline{X}_i + (C_i + \delta C_i)] \end{aligned} \tag{6}$$

where $\delta\mathbf{A}_i = \mathrm{diag}(\delta A_1, \delta A_2, \delta A_1)$ is an unknown bounded diagonal-matrix disturbance, $\delta\mathbf{B}_i$ is an unknown bounded matrix disturbance, and δC_i is an unknown bounded vector disturbance. Hence, the derivative of (4) with parametric uncertainties becomes

$$\dot{V}|_{(6)} = -\left[X_e^T(\overline{\mathbf{A}}_i X_i + \overline{C}_i) + X_e^T \overline{\mathbf{B}}_i u\right] = -[f(u) + \delta f(u)] \equiv \overline{f}(u) \tag{7}$$

where $\delta f(u) = X_e^T(\delta\mathbf{A}_i X_i + \delta C_i) + X_e^T \delta\mathbf{B}_i u$ is unknown. Suppose that $\delta f(u)$ is bounded and there exists a positive value C_M, such that

$$\delta f(u) < C_M \|X_e\|^2 \tag{8}$$

where $\|x\|^2$ is defined as the 2-norm value of vector x. From (7) and (8), it follows that

$$\overline{f}(u) - C_M \|X_e\|^2 < f(u). \tag{9}$$

Expression (9) implies that $\overline{f}(u) - C_M\|X_e\|^2$ is a lower-bound of $f(u)$. If $\overline{f}(u) - C_M\|X_e\|^2 > 0$ can be guaranteed, then $f(u) > 0$ is satisfied and thus the system has the robust property w.r.t. the parametric uncertainties.

Choose the controller u in (2) with parametric uncertainties such that

$$u = \overline{\mathbf{B}}_i^{-1}(\overline{\mathbf{K}}_g X_e - \overline{\mathbf{A}}_i \overline{X}_i - \overline{C}_i) \tag{10}$$

where $\overline{\mathbf{K}}_g = \mathrm{diag}(\alpha_1 + \overline{A}_1, \alpha_2 + \overline{A}_2, \alpha_3 + \overline{A}_1)$, and $(\overline{A}_1, \overline{A}_2, \overline{A}_1)$ are the diagonal elements of matrix $\overline{\mathbf{A}}_i$. Substituting (10) into (7) yields

$$\dot{V}|_{(6)} = -\overline{f}(u) = -\left[X_e^T(\overline{\mathbf{K}}_g - \overline{\mathbf{A}}_i) X_e\right] \equiv -X_e^T \mathbf{Q} X_e \tag{11}$$

where $\mathbf{Q} = \overline{\mathbf{K}}_g - \overline{\mathbf{A}}_i = \mathrm{diag}(\alpha_1, \alpha_2, \alpha_3) > 0$ is a symmetric positive-definite (SPD) matrix. From (9) and (11), it is clear that

$$[\lambda_{\min}(\mathbf{Q}) - C_M]\|X_e\|^2 \le \overline{f}(u) - C_M\|X_e\|^2 < f(u) \tag{12}$$

where $\lambda_{\min}(\mathbf{Q}) = \min(\alpha_1, \alpha_2, \alpha_3)$ denotes the minimum eigenvalue of matrix $\mathbf{Q}$. Expression (12) shows that if $\lambda_{\min}(\mathbf{Q})$ is larger than C_M defined in (8), then $\overline{f}(u) - C_M\|X_e\|^2 > 0$ is guaranteed. This means the proposed visual tracking controller (2) is robust against the unknown parametric uncertainties. Summarizing the previous discussions, we obtain the following theorem.

Theorem 1: Consider the visual interaction model (1) with unknown bounded parametric uncertainties $\delta\mathbf{A}_i$, $\delta\mathbf{B}_i$, and δC_i defined in (6). Let C_M be a positive value defined in (8). Choosing the controller u as given in expression (2) with parameters $(\alpha_1, \alpha_2, \alpha_3) > 0$, the closed-loop visual tracking control system is asymptotically stable for all $\alpha_i > C_M$, $i = 1 \sim 3$. ■

In Section V, the result of *Theorem 1* will be validated by practical experiments. Further, in realization of the control schemes, it was noted that the quantization error in velocity commands degrade the performance of the controller and might make the system unstable. It is, therefore, interesting to study the robustness issues related to velocity quantization uncertainty. In Section IV, a robust control law based on Lyapunov's direct method will be derived to overcome the velocity quantization uncertainty in practical control systems. A general form to describe the bounded uncertainty term $\delta f(u)$ should be that $\delta f(u) < C_M\|X_e\|^2 + C_N\|X_e\|$, where C_M and C_N are two positive values. In this paper, we ignore the effect from the second term $C_N\|X_e\|$ and leave it in the future work.

IV. Robustness Against Velocity Quantization Error

When tracking a target, it is desirable for the robot to have a smooth motion in human-robot interaction. But in such circumstances, one will face the problem caused by velocity quantization error in practical implementation. In this section, a robust control law is derived to handle the velocity quantization error encountered in practical control systems based on the error-state model defined in (5). To do so, a stability necessary condition (SNC) is first derived for ensuring global asymptotic stability of the closed-loop visual tracking system through Lyapunov's direct method. The robust control law is then proposed to guarantee that the visual tracking system satisfies the SNC and hence complete the controller design.A.

A. Stability Necessary Condition

Digital control systems usually have *uniform* quantization errors due to finite-length effects on sampled values [17]. In other words, the ideal (theoretical) control command u is quantized such that

$$\overline{u} = u + \delta u \tag{13}$$

where $\overline{u}$ denotes the practical (actual) control command sent to the robot actuator, and $\delta u = [\,\delta v_f^m \quad \delta w_f^m \quad \delta w_t^m\,]^T$ represents the uniform quantization error encountered in the system. Thus, in practice, (7) becomes

$$\dot{V}|_{(6),(13)} = -\overline{f}(\overline{u}) = -[\overline{f}(u) + \delta\overline{f}(\delta u)] = \dot{V}|_{(6)} - \delta\overline{f}(\delta u) \tag{14}$$

where $\delta\overline{f}(\delta u) = X_e^T \overline{\mathbf{B}}_i \delta u$. Expression (14) implies that even if u satisfies $\overline{f}(u) - C_M\|X_e\|^2 > 0$, the practical control system still can be unstable caused by $\delta\overline{f}(\delta u) < 0$. Therefore, one has the following SNC in practical control implementation.

> *SNC*: Let δu denote the velocity output quantization error in practical systems. Consider the visual interaction model (1) with unknown bounded parametric uncertainties. Choose a control law u that satisfies $\overline{f}(u) - C_M\|X_e\|^2 > 0$ defined in (7) and (8). If $\delta\overline{f}(\delta u) = X_e^T \overline{\mathbf{B}}_i \delta u \ge 0$ is satisfied. Then, the system state in practical system achieves asymptotic convergence under the condition $\delta\overline{f}(\delta u) = X_e^T \overline{\mathbf{B}}_i \delta u \ge 0$. ■

B. Proposed Robust Control Law

SNC implies that a practical system may become unstable if $\delta\overline{f}(\delta u) < 0$ satisfies. Our goal is to design a robust control law that not only guarantees SNC to be always satisfied but also increases the convergence rate of the control system. First, we expand $\delta\overline{f}(\delta u)$ such that

$$\delta\overline{f}(\delta u) = \gamma_1 \delta v_f^m + \gamma_2 \delta w_f^m + \gamma_3 \delta w_t^m \tag{15}$$

where $\gamma_1 = \overline{B}_{11}x_e + \overline{B}_{21}y_e + \overline{B}_{31}d_e$, $\gamma_2 = \overline{B}_{12}x_e + \overline{B}_{22}y_e + \overline{B}_{32}d_e$, $\gamma_3 = \overline{B}_{13}x_e + \overline{B}_{23}y_e + \overline{B}_{33}d_e$, and $\overline{B}_{mn}$ denotes the element of matrix $\overline{\mathbf{B}}_i$ corresponding to the mth row and nth column. Next, based on the velocity transformation $v_l^m = v_f^m - (D \cdot w_f^m)/2$ and $v_r^m = v_f^m + (D \cdot w_f^m)/2$, where v_l^m and v_r^m are, respectively, left and right wheel velocities, and D represents the distance between two drive wheels, expression (15) becomes

$$\delta\overline{f}(\delta u) = \left[\left(\frac{\gamma_1}{2}\right) + \left(\frac{\gamma_2}{D}\right)\right]\delta v_r^m + \left[\left(\frac{\gamma_1}{2}\right) - \left(\frac{\gamma_2}{D}\right)\right]\delta v_l^m + \gamma_3 \delta w_t^m \tag{16}$$

where $\delta v_l^m = \delta v_f^m - (D \cdot w_f^m)/2$ and $\delta v_r^m = \delta v_f^m + (D \cdot w_f^m)/2$ are the uniform quantization error encountered in left and right wheel velocities, respectively. Expression (16) reveals that if each term in (16) is equal to a nonnegative value, then $\delta\overline{f}(\delta(u)) \geq 0$ can be guaranteed. Based on this idea, a variable structure robust control law is derived such that

$$\begin{aligned}
&\text{If } \left[\left(\frac{\gamma_1}{2}\right) + \left(\frac{\gamma_2}{D}\right)\right]\delta v_r^m < 0, \text{ then} \\
&\qquad \overline{v}_r^{m*} = \begin{cases} \overline{v}_r^m - \varepsilon_r, & \text{if } \delta v_r^m > 0 \\ \overline{v}_r^m + \varepsilon_r, & \text{if } \delta v_r^m < 0 \end{cases} \\
&\qquad \text{end if.} \\
&\text{If } \left[\left(\frac{\gamma_1}{2}\right) - \left(\frac{\gamma_2}{D}\right)\right]\delta v_l^m < 0, \text{ then} \\
&\qquad \overline{v}_l^{m*} = \begin{cases} \overline{v}_l^m - \varepsilon_l, & \text{if } \delta v_l^m > 0 \\ \overline{v}_l^m + \varepsilon_l, & \text{if } \delta v_l^m < 0 \end{cases} \\
&\qquad \text{end if.} \\
&\text{If } \gamma_3 \delta w_t^m < 0, \text{ then} \\
&\qquad \overline{w}_t^{m*} = \begin{cases} \overline{w}_t^m - \varepsilon_t, & \text{if } \delta w_t^m > 0 \\ \overline{w}_t^m + \varepsilon_t, & \text{if } \delta w_t^m < 0 \end{cases} \\
&\qquad \text{end if}
\end{aligned} \tag{17}$$

where $(\overline{v}_l^{m*}, \overline{v}_r^{m*}, \overline{w}_t^{m*})$ are the outputs of the proposed robust control law for tracking control of the robot, and $(\varepsilon_l, \varepsilon_r, \varepsilon_t)$ are three positive constants such that

$$(\varepsilon_l, \varepsilon_r, \varepsilon_t) = (\sup|\delta v_l^m|, \sup|\delta v_r^m|, \sup|\delta w_t^m|). \tag{18}$$

The value of constants $(\varepsilon_l, \varepsilon_r, \varepsilon_t)$ is calculated based on the range of quantization errors $(\delta v_l^m, \delta v_r^m, \delta w_t^m)$ that are dependent on the resolution of robot motion control module. It is easy to show that the outputs of the proposed robust control law guarantee that each term of (16) is equal to a nonnegative value, and thus SNC is satisfied. Further, because of $\dot{V}|_{(6),(13)} = \dot{V}|_{(6)} - \delta\overline{f}(\delta u) \leq \dot{V}|_{(6)} < 0$, an increase of the convergence rate of the practical system is obtained. In Section V, the stability characteristic and convergence performance of the proposed control law will be verified by two practical experiments.

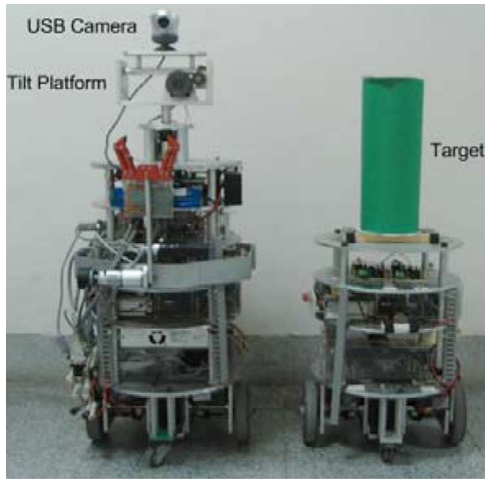

Fig. 5. Experimental mobile robots used to test the tracking performance of the proposed visual tracking control method. Left robot is called tracking robot and right one is called target robot.

Remark 3: Although quantization errors are analyzable using techniques developed for finite word-length controllers [18], the previous reported methods are only useful for linear time-invariant (LTI) systems, but not suitable for Quasi-LPV systems. On the contrary, our proposed control method can be applied to both LTI and Quasi-LPV systems. This is the merit of the proposed method. On the other hand, adding an integral term in the proposed linear controller or using a more responsive controller with high control gain can be effective to reduce the effect of quantization error; however, these methods usually generate large control outputs. In many applications in human-centered service robotics, one expects relatively smooth motion for safety considerations. The proposed control method with smaller control gain guarantees that the equilibrium point of practical system is also asymptotically stable with improved convergence performance.

V. Experimental Results

Fig. 5 shows the experimental mobile robots used to test the tracking performance of the proposed visual tracking control method. Left robot (called *tracking robot*) is equipped with a USB camera and a tilt camera platform to track another robot (called *target robot*) on which a target of interest was installed. Two experiments have been carried out to verify the performance of the proposed control schemes: the first experiment aims to validate the robustness against the uncertainty of velocity quantization error, and the second one is to verify the result of *Theorem 1*. The parameters used in the experiments are listed in Table I. Note that different control gains were used in the second experiment in order to verify *Theorem 1*.

A. Experiment 1: Robustness to Velocity Quantization Error

In this experiment, the target is set static in order to validate the performance of the proposed robust control law (17). Since the target is static $\left(V_f^t = 0\right)$, the controller (2) is simplified to $u = \mathbf{B}_i^{-1}\mathbf{K}_g X_e$ due to $\mathbf{A}_i = 0$ and $C_i = 0$. Fig. 6 presents the experimental results using the simplified controller without the proposed robust control law (17). Fig. 6(a) indicates the tracking

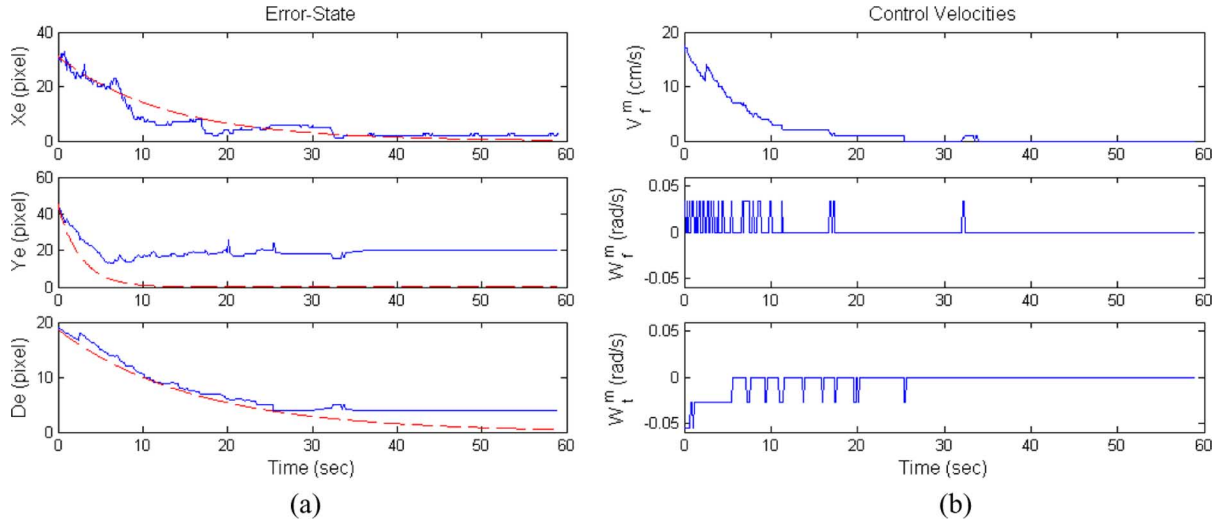

Fig. 6. Experimental results of the experiment 1 without using the proposed robust control law (17). (a) Tracking errors in the image plane. (b) Control velocities of the center point and tilt camera of tracking robot.

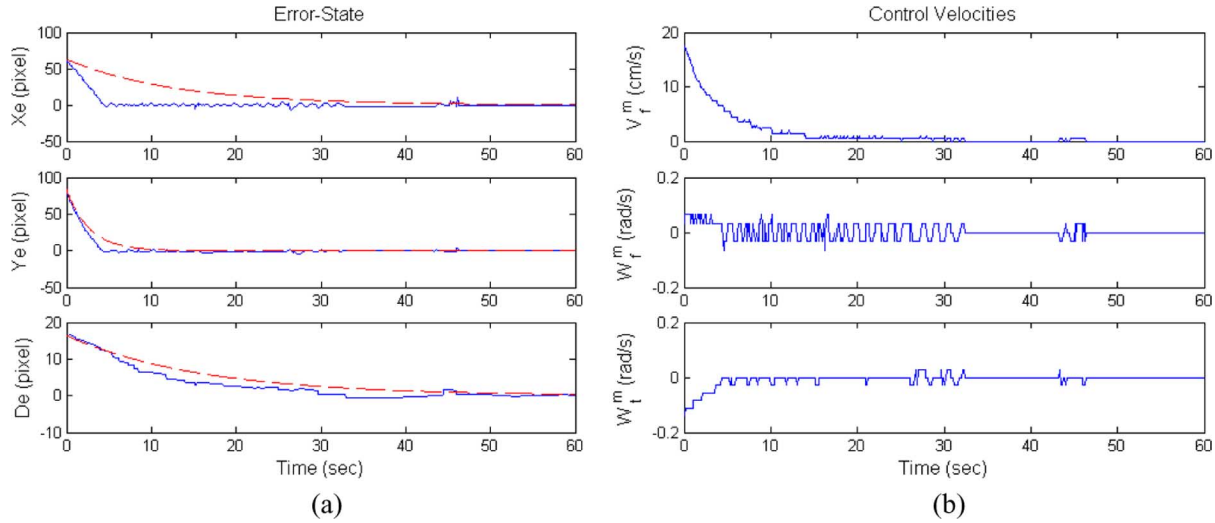

Fig. 7. Experimental results of the experiment 1 using the proposed robust control law (17). (a) Tracking errors in the image plane. (b) Control velocities of the center point and tilt camera of tracking robot.

errors in the image plane, in which the dotted lines are the simulated theoretical values and the solid lines are the recorded experimental values. From Fig. 6(a), we see that the system state in the practical experiment do not converge to the desired states. This is mainly caused by the system quantization error in the velocity commands, which degrades the performance of the controller. Fig. 6(b) shows the control velocities of the tilt camera and the tracking robot. In Fig. 6(b), it can be seen that the angular velocity of the robot is smaller than 0.04 rad/s; the quantization error greatly affects the actual angular velocity under such small values. Consequently, the system state cannot converge to the desired state as desired.

We repeated then the experiment by combining the proposed robust control law (17) with the visual tracking controller. When the velocity quantization noise is uniform, each quantitative level has the same quantization effect, and the proposed control law (17) is robust to this uncertainty.

Fig. 7 presents the experimental results using the simplified controller with the robust control law (17). Fig. 7(a) indicates the tracking errors in the image plane. We see that the convergence rate of experimental results is faster than that of theoretical ones. This verifies that the proposed robust control law not only guarantees the tracking errors to decay to zero asymptotically but also increases the convergence rate of the practical system. Fig. 7(b) shows the control velocities of the tracking robot. A video clip of the experiment 1 by combining the proposed robust control law with the simplified visual tracking controller is available online.[1]

B. Experiment 2: Robustness to System Model Uncertainty

In this experiment, the target as shown in Fig. 2 was installed on top of a mobile robot for another robot to track. The target mobile robot was set to move along a circular path with velocities $\left(v_f^x, v_f^y, v_f^z\right) = \left(v_f^t \sin\left(\pi + T_t w_f^t\right),\ 0, v_f^t \cos\left(\pi + T_t w_f^t\right)\right)$, where $v_f^t =$

[1][Online]. Available: http://isci.cn.nctu.edu.tw/video/RVTC_T/Static.wmv

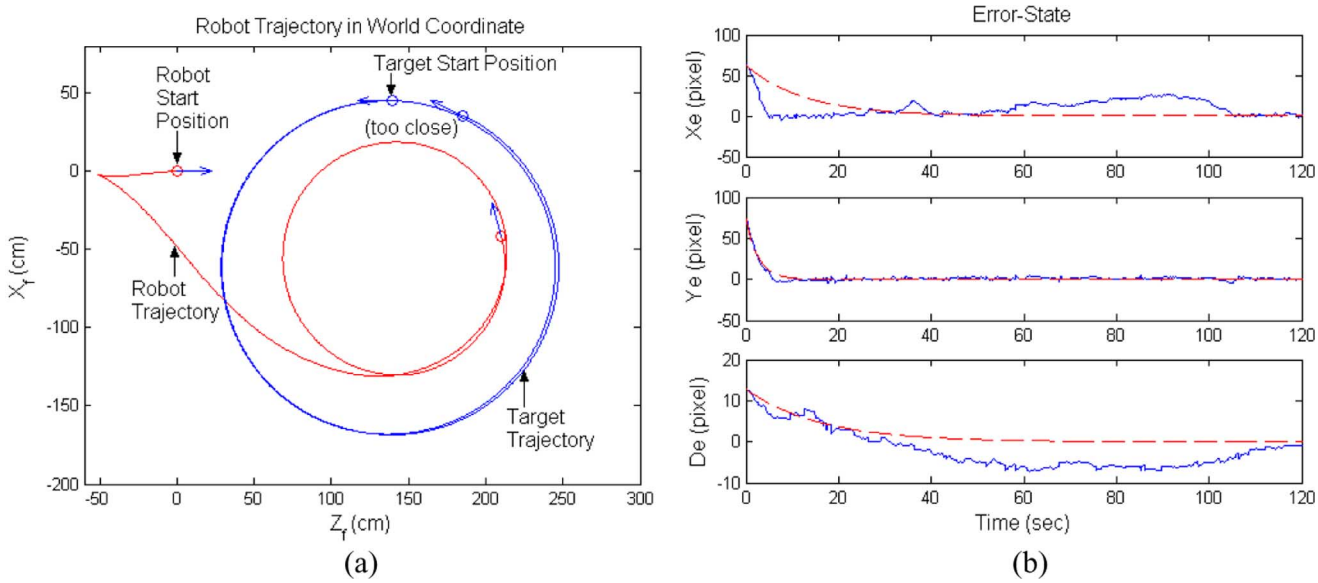

Fig. 8. Experimental results of the experiment 2 with control gains (5/64,6/16,4/64). (a) Robot trajectory in world coordinates. (b) Tracking errors in the image plane.

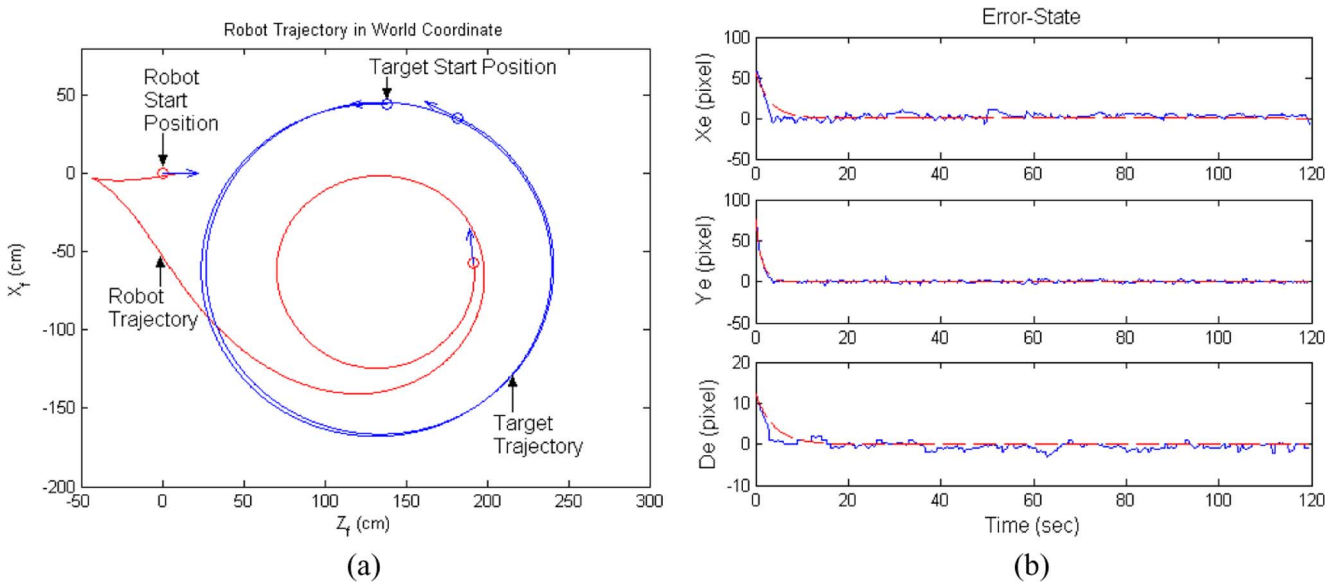

Fig. 9. Experimental results of the experiment 2 with larger control gains (5/16,6/8,4/16). (a) Robot trajectory in world coordinates. (b) Tracking errors in the image plane.

10.5 cm/s, $w_f^t = 0.1$ rad/s, and $T_t = 51$ ms. In order to validate *Theorem 1*, small control gains $\left(\alpha_1^S, \alpha_2^S, \alpha_3^S\right)$ were first applied to the control law (2), which implies a small robustness against the system parametric uncertainties. Later, larger control gains $\left(\alpha_1^L, \alpha_2^L, \alpha_3^L\right)$ were used in order to increase the robustness and improve the tracking performance of the closed-loop visual tracking system.

Fig. 8 presents the recorded responses of this experiment using small control gains $\left(\alpha_1^S, \alpha_2^S, \alpha_3^S\right)$. In Fig. 8(a), the trajectories of the tracking robot and the target robot were recorded in world coordinates. Both trajectories were recorded by counting the pulses from shaft encoders. Fig. 8(b) depicts the tracking errors in the image plane. In Fig. 8(a), we observe that the tracking robot followed the target with a poor performance, which also can be seen in Fig. 8(b). In Fig. 8(b), the error states x_e and d_e in the experiment do not converge to zero asymptotically. The reason is that the closed-loop visual tracking system is asymptotically stable only for $\min\left(\alpha_1^S, \alpha_2^S, \alpha_3^S\right) > C_M$ in the experiment. This implies that the proposed controller provided a modest robustness of tracking errors against the parametric uncertainties.

According to *Theorem 1*, the proposed controller with larger control gains provides better robust property w.r.t. the system parametric uncertainties. Hence, larger control gains $\left(\alpha_1^L, \alpha_2^L, \alpha_3^L\right)$ as listed in Table I were used to repeat the experiment. Fig. 9 shows the recorded responses of this experiment. In Fig. 9(a), it is clear that the tracking robot tracked the target in a circular motion with improved performance compared with that of Fig. 8. Fig. 9(b) depicts the tracking errors in the image plane. We see that the system state in the experiment

TABLE I
PARAMETERS USED IN THE EXPERIMENTS

Symbol	Values	Description
(f_x, f_y)	(294,312) pixels	Camera focal length in retinal coordinates.
W	12 cm	Width of the target.
D	30 cm	Distance between two drive wheels.
$(\overline{x}_i, \overline{y}_i, \overline{d}_x)$	(0,0,35)	Desired system state in the image plane.
$(\alpha_1^S, \alpha_2^S, \alpha_3^S)$	(5/64,6/16,4/64)	Control gains of experiment 1 and 2
$(\alpha_1^L, \alpha_2^L, \alpha_3^L)$	(5/16,6/8,4/16)	Control gains of experiment 2
$(\varepsilon_l, \varepsilon_r, \varepsilon_t)$	(1,1,0.028)	Max. quantization errors
$(z_f^m, x_f^m, \theta_f^m, \phi)\|_{t=0}$	(0,0,0,0)	Initial pose of the tracking robot.

converges asymptotically to the desired state as expected. These experimental results verify *Theorem 1* and the robust control law (17) as well. A video clip of the experiment 2 by using the proposed visual tracking controller with larger control gains $\left(\alpha_1^L, \alpha_2^L, \alpha_3^L\right)$ is available online.[2]

VI. CONCLUSION AND FUTURE WORK

A study of system model and velocity quantization uncertainties in visual tracking control of a wheeled mobile robot has been presented in this paper. In the parametric robustness analysis, we have shown that the proposed visual tracking controller is robust w.r.t. system model uncertainties. Moreover, based on Lyapunov theory, the robust control law efficiently overcomes the unmodeled quantization effect in the velocity commands. Experimental results validate that the proposed control schemes guarantee asymptotic stability of the visual tracking system with parametric and velocity quantization uncertainties. In the future, we will extend this work to the general case of any task/command dimension such as a mobile-manipulator system.

ACKNOWLEDGMENT

The authors would like to thank the Associate Editor, Prof. B. de Jager, and the anonymous reviewers for their helpful comments and suggestions.

REFERENCES

[1] F. Conticelli, B. Allotta, and P. K. Khosla, "Image-based visual servoing of nonholonomic mobile robots," in *Proc. IEEE 38th Conf. Decision Control*, Phoenix, AZ, 1999, pp. 3496–3501.

[2] Y. Ma, J. Košecká, and S. S. Sastry, "Vision guided navigation for a nonholonomic mobile robot," *IEEE Trans. Robot. Autom.*, vol. 15, no. 3, pp. 521–536, 1999.

[3] H. Zhang and J. P. Ostrowski, "Visual motion planning for mobile robots," *IEEE Trans. Robot. Autom.*, vol. 18, no. 2, pp. 199–208, Feb. 2002.

[2][Online]. Available: http://isci.cn.nctu.edu.tw/video/RVTC_T/Circular.wmv

[4] D. Burschka, J. Geiman, and G. Hager, "Optimal landmark configuration for vision-based control of mobile robot," in *Proc. IEEE Int. Conf. Robot. Autom.*, Taipei, Taiwan, 2003, pp. 3917–3922.

[5] Y. Fang, W. E. Dixon, D. M. Dawson, and P. Chawda, "Homography-based visual servo regulation of mobile robots," *IEEE Trans. System, Man, Cybern.-Part B: Cybern.*, vol. 35, no. 5, pp. 1041–1049, May 2005.

[6] J. Chen, W. E. Dixon, D. M. Dawson, and M. McIntyre, "Homography-based visual servo tracking control of a wheeled mobile robot," *IEEE Trans. Robot.*, vol. 22, no. 2, pp. 407–416, Apr. 2006.

[7] G. L. Mariottini, D. Prattichizzo, and G. Oriolo, "Epipole-based visual servoing for nonholonomic mobile robots," in *Proc. IEEE Int. Conf. Robot. Autom.*, New Orleans, LA, 2004, pp. 497–503.

[8] G. López-Nicolás, C. Sagüés, J. J. Guerrero, D. Kragic, and P. Jensfelt, "Nonholonomic epipolar visual servoing," in *Proc. IEEE Int. Conf. Robot. Autom.*, Orlando, FL, 2006, pp. 2378–2384.

[9] H. Y. Wang, S. Itani, T. Fukao, and N. Adachi, "Image-based visual adaptive tracking control of nonholonomic mobile robots," in *Proc. IEEE/RSJ Int. Conf. Intel. Robot. Syst.*, Maui, HI, 2001, pp. 1–6.

[10] K.-T. Song and C.-C. Chien, "Visual tracking of a moving person for a home robot," *J. Systems Control Eng.*, vol. 219, no. 14, pp. 259–269, 2005.

[11] E. Malis and S. Benhimane, "A unified approach to visual tracking and servoing," *J. Robot. Autonomous Syst.*, vol. 52, no. 1, pp. 39–52, 2005.

[12] Y. Han and H. Hahn, "Visual tracking of a moving target using active contour based SSD algorithm," *Robot. Autonomous Syst.*, vol. 53, no. 3-4, pp. 265–281, 2005.

[13] C.-Y. Tsai and K.-T. Song, "Face tracking interaction control of a nonholonomic mobile robot," in *Proc. IEEE/RSJ Int. Conf. Intell. Robots Syst.*, Beijing, China, pp. 3319–3324.

[14] C.-Y. Tsai, K.-T. Song, X. Dutoit, H. Van Brussel, and M. Nuttin, "Robust mobile robot visual tracking control system using self-tuning Kalman filter," in *Proc. IEEE Int. Symp. Computational Intell. Robot. Autom.*, Jacksonville, FL, 2007, pp. 161–166.

[15] W. J. Rugh and J. S. Shamma, "Survey paper: Research on gain scheduling," *Automatica*, vol. 36, no. 10, pp. 1401–1425, 2000.

[16] J.-J. E. Slotine and W. Li, *Applied Nonlinear Control*. Englewood Cliffs, NJ: Prentice-Hall, 1991.

[17] A. V. Oppenheim and R. W. Schafer, *Discrete-Time Signal Processing*. Upper Saddle River, NJ: Prentice-Hall, 1999.

[18] K. Liu, R. E. Skelton, and K. Grigoriadis, "Optimal controllers for finite word length implementation," *IEEE Trans. Autom. Control*, vol. 37, no. 9, pp. 1294–1304, Sep. 1992.

Chi-Yi Tsai was born in Kaohsiung, Taiwan, in 1978. He received the B.S. and M.S. degrees in electrical engineering from National Yunlin University of Science and Technology, Yunlin, Taiwan, in 2000 and 2002, respectively. He is currently pursuing the Ph.D. degree in electrical and control engineering from the National Chiao Tung University, Taiwan.

Currently, he is an Engineer with the Software R&D Department, EPC Business Unit, ASUSTek Computer Incorporation, Taipei, Taiwan. His research interests include image processing, color enhancement processing, visual tracking control of the mobile robot, visual servoing, and computer vision.

Kai-Tai Song (A'91) was born in Taipei, Taiwan, in 1957. He received the B.S. degree in power mechanical engineering from National Tsing Hua University, Taiwan, in 1979, and the Ph.D. degree in mechanical engineering from the Katholieke Universiteit Leuven, Leuven, Belgium, in 1989.

Since 1989, he has been on the faculty and is currently a Professor with the Department of Electrical and Control Engineering, National Chiao Tung University, Taiwan. He was with Chung Shan Institute of Science and Technology from 1981 to 1984. His research interests include mobile robots, image processing, visual tracking, sensing and perception, embedded systems, intelligent system control integration, and mechatronics. He served as the chairman of the Society of IEEE Robotics and Automation, Taipei Chapter from 1998 to 1999.